A Cyclic Antimicrobial Peptide Produced in Primate Leukocytes by the Ligation of Two Truncated α-Defensins

Yi-Quan Tang,[1] Jun Yuan,[1] George Ösapay,[1] Klara Ösapay,[1] Dat Tran,[1] Christopher J. Miller,[2] Andre J. Ouellette,[1] Michael E. Selsted[1]*

Analysis of rhesus macaque leukocytes disclosed the presence of an 18-residue macrocyclic, tridisulfide antibiotic peptide in granules of neutrophils and monocytes. The peptide, termed rhesus theta defensin-1 (RTD-1), is microbicidal for bacteria and fungi at low micromolar concentrations. Antibacterial activity of the cyclic peptide was threefold greater than that of an open-chain analog, and the cyclic conformation was required for antimicrobial activity in the presence of 150 millimolar sodium chloride. Biosynthesis of RTD-1 involves the head-to-tail ligation of two α-defensin–related nonapeptides, requiring the formation of two new peptide bonds. Thus, host defense cells possess mechanisms for synthesis and granular packaging of macrocyclic antibiotic peptides that are components of the phagocyte antimicrobial armamentarium.

Antimicrobial peptides are evolutionarily ancient elements of innate immunity (1). Mammalian defensins, comprising genetically distinct α and β subfamilies, are cationic, tridisulfide peptides of 29 to 42 amino acids length that possess potent broad-spectrum microbicidal activities in vitro (2). Many defensins appear to be expressed constitutively, whereas the biosynthesis of others is induced by mediators of inflammation (3). Neutrophil α-defensins are packaged in azurophil granules that are mobilized during phagocytosis for delivery to phagosomes containing ingested microbes. In vitro studies demonstrate that defensins kill microorganisms by permeabilizing one or more target cell membranes (4).

We undertook studies to characterize defensin expression in the leukocytes of rhesus macaques. In addition to several α-defensins isolated from monkey neutrophils, we isolated a tridisulfide-containing antimicrobial peptide, termed rhesus theta defensin 1 (RTD-1), in which the peptide backbone is naturally cyclized.

Isolation and characterization of RTD-1. RTD-1 was isolated from rhesus macaque leukocytes [>90% polymorphonuclear (PMN)] by reversed-phase (RP) high-performance liquid chromatography (HPLC) of a whole-cell extract enriched for α-defensins (Fig. 1) (5).

Chromatographic peaks eluting between 20 and 50 min were purified to homogeneity and screened for antibacterial activity against *Escherichia coli* ML35 and *Staphylococcus aureus* 502a (6), and microbicidal peptides were characterized by amino acid analysis and automated Edman degradation (7). Seven of the eight purified antimicrobial peptides were α-defensins that were similar in sequence and activity to orthologous human peptides (8). RTD-1

(arrow in Fig. 1A) was relatively abundant and possessed the greatest antibacterial activity of any of the peptides isolated. The yield of RTD-1 was ~100 μg per 10^9 neutrophils.

Amino acid analysis of RTD-1 revealed that it was composed of 18 amino acids: 1 Thr, 1 Val, 1 Leu, 1 Phe, 1 Ile, 2 Gly, 5 Arg, and 6 Cys. MALDI-TOF MS analysis (9) of the native (2082.0) and *S*-pyridylethylated (10) (2720.3) peptides demonstrated that the six cysteines exist as three intramolecular disulfides. Because the peptide's apparent NH₂-terminus was blocked, the primary structure of RTD-1 was determined by sequencing overlapping fragments produced by methanolic-HCl treatment (11) and digestion with chymotrypsin and trypsin (12) (Fig. 2A). These analyses revealed that the RTD-1 backbone is cyclized through peptide bonds (Fig. 2B). The cyclic conformation accounts for the 18 atomic mass unit difference (equal to one water molecule) between the measured mass (2082.0; 2081.6 calculated) of RTD-1 and that of a linear tridisulfide peptide (2099.6 calculated) of the same composition.

The disulfide structure of RTD-1 was determined by characterizing protease digestion fragments produced by sequential incubation of native peptide with trypsin and thermolysin (13). Following trypsin digestion, a major product was purified by HPLC and its mass was determined to be 1998.1. Comparison of the mass and amino acid analysis of this peptide revealed that it was produced by cleavage at the COOH side of all five arginine residues, thus generating a 17-residue oligopeptide (or 17-mer) composed of four peptides linked by three disulfides (calculated mass = 1997.5; Fig. 2C).
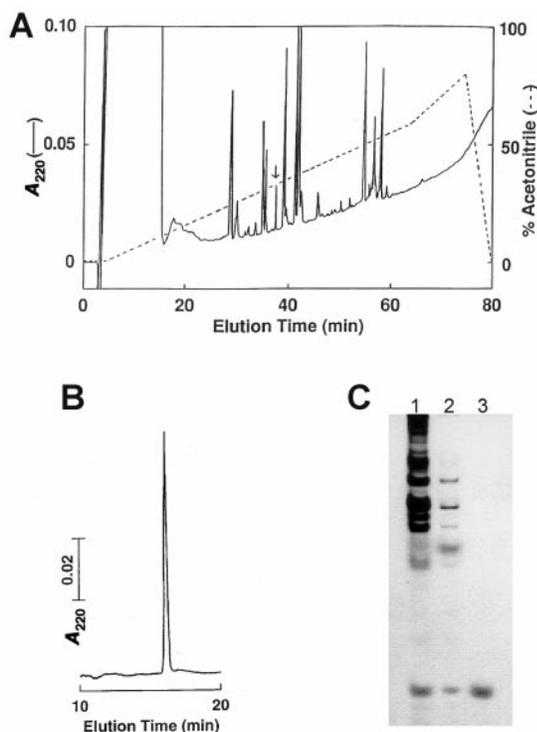

Fig. 1. Purification of RTD-1. (**A**) RP-HPLC of peripheral blood leukocyte extracts. An α-defensin-enriched extract of 6 × 10^6 leukocytes (91% PMNs) (8) was fractionated by RP-HPLC on a 0.46 × 25 cm C-18 column equilibrated in 0.1% aqueous TFA and developed with a linear acetonitrile gradient (dotted line). RTD-1 eluted in the arrow-marked peak. (**B**) Analytical RP-HPLC of purified RTD-1. The purity of RTD-1 was assessed by RP-HPLC of RTD-1 obtained from the peak (arrow) in (A) on an analytical C-18 column equilibrated in aqueous 0.13% HFBA and developed with a linear (20 to 60%) acetonitrile gradient in 20 min. (**C**) Acid-urea PAGE. Samples of 30% acetic acid granulocyte extract (2 × 10^6 cell equivalents; lane 1), the subsequent methanol:water extract (1 × 10^7 cell equivalents; lane 2), and 0.4 μg of RTD-1 were resolved on a 12.5% acid-urea polyacrylamide gel and stained with formalin-Coomassie blue.

[1]Department of Pathology, College of Medicine, University of California, Irvine, CA 92697, USA. [2]California Regional Primate Research Center and Center for Comparative Medicine, School of Veterinary Medicine, University of California, Davis, CA 95616, USA.

*To whom correspondence should be addressed. E-mail: meselste@uci.edu

To distinguish between the eight possible disulfide pairings in the 17-mer, the oligopeptide was digested with thermolysin and the resulting fragments were analyzed by MALDI-TOF MS (*9*). The *m/z* values of the thermolysin fragments were consistent with only one cystine motif (Fig. 2C), revealing that the peptide ring is stabilized by three disulfides in a picket fence–like array that crosslinks two hypothetical β-strands connected by turns at both ends (Fig. 2, D and E). Schematically, RTD-1 resembles the Greek letter theta (Fig. 2D), hence the selection of θ-defensin to describe this molecular motif. The peptide is highly cationic, possessing a net charge of +5 at pH 7 (calculated pI > 12), and the dense cystine motif is distinct from that determined for α- or β-defensins (*14*).

The structure and activities of RTD-1 were confirmed by the preparation and characterization of synthetic RTD-1. The purified synthetic product was identical to natural RTD-1 as determined by RP-HPLC, acid-urea polyacrylamide gel electrophoresis (PAGE), circular dichroism spectroscopy, disulfide motif, and quantitative microbicidal activity [supplemental figures 1 and 2 (*15*)]. Together these data confirm the structure and biological activity of native RTD-1.

Searches for amino acid sequence similarity to RTD-1 were carried out using all 18 possible linearized peptides as query sequences (*16*). Taking into consideration the cysteine spacing and disulfide connectivities of RTD-1, the most similar polypeptide sequence identified was that of protegrin-3 (PG-3), an antimicrobial peptide from pig neutrophils (*17*). Protegrins are 17- to 18–amino acid, bis-disulfide–containing peptides that are members of the cathelicidin family of antimicrobial peptides (*18*). Like protegrins, RTD-1 is predicted to be predominantly composed of two disulfide-stabilized β-strands connected by turns. A model of RTD-1, derived from molecular dynamics simulations (Fig. 2E) (*19*), is remarkably similar to the solution structure of protegrin-1 (PG-1), an isoform of PG-3. Despite this similarity, cloning experiments revealed that RTD-1 is not a rhesus cathelicidin.

The occurrence of RTD-1 in primate phagocytes discloses a structural motif in animals resembling a group of macrocyclic peptides previously characterized in plants. Like RTD-1, cyclic peptides isolated from plants of the Rubiaceae family molecules possess three intramolecular disulfides (*20*). Two of these peptides are reported to be antiviral against HIV-1 (*21*). The plant peptides differ from RTD-1 in their size (29 to 31 versus 18 amino acids, respectively) and they contain a cystine motif that is characterized by "overlapping" disulfides that produce a cystine knot (*22*). Thus far, the genes encoding these plant peptides have not been reported, nor have mechanisms been proposed for the formation of the cyclic backbone. The only other macrocyclic peptides that we are aware of lack disulfides. One, AS-48, is a plasmid-encoded peptide expressed by *Enterococcus faecalis* (*23*); the second is J25, a microcin from *E. coli* (*24*).

Cloning of RTD-1 precursors. To elucidate the RTD-1 biosynthetic pathway, we sought to characterize the peptide precursor by analysis of one or more of the corresponding cDNAs from rhesus macaque bone marrow mRNA. Because the NH_2-terminus of RTD-1 could not be predicted from its cyclic sequence, we conducted 3′ RACE (rapid amplification of cDNA ends) experiments using degenerate oligonucleotide primers corresponding to six to seven amino acid segments of the peptide sequence (*25*). These amplifications consistently yielded two sequences that separately corresponded to different portions of RTD-1: R^8-R^9-G^{10}-V^{11}-C^{12}-[Q-L-L-stop] and T^{17}-R^{18}-G^1-F^2-C^3-[R-L-L-stop] (Fig. 2D) (*25*). The 3′ RACE products were then used to probe a rhesus macaque bone marrow cDNA library (*26*). Fifteen positive clones were isolated and sequenced, revealing two highly similar cDNAs (92% identity) termed RTD1a and RTD1b (Genbank accession numbers AF191100 and AF191101, respectively). Surprisingly, none of the clones analyzed contained a sequence that coded for all 18 amino acids in RTD-1.

RTD1a and RTD1b each encode 76–amino acid pre-propeptides containing a 20-residue signal peptide and a 44–amino acid prosegment, which are identical in size and

Fig. 2. Peptide backbone structure of RTD-1. (**A**) The amino acid sequence of the peptide chain was determined by Edman sequencing or MALDI-TOF MS, or both, of fragments produced by methanolic-HCl treatment or digestion with chymotrypsin (CT) and trypsin (T). Disulfides were reduced with dithiothreitol and alkylated with 4-vinyl pyridine before digestion so that cysteines were analyzed as *S*-pyridylethyl cysteine. Residues in parentheses were assigned based on MALDI-TOF MS data. Calculated MALDI-TOF MS values are in parentheses. (**B**) Amino acid sequence of the RTD-1 peptide backbone. (**C**) Disulfide analysis of RTD-1. A tridisulfide-containing 17-residue oligopeptide generated by trypsin digestion was purified by RP-HPLC and digested further with thermolysin (*13*). MS analyses (calculated values in parentheses) of the digest disclosed thermolytic cleavage at Cys-14/Ile-15 and at Cys-5/Leu-6 (arrows), producing four major thermolytic fragments (Th-1 to Th-4). The masses of all fragments from several digests were uniquely consistent with the disulfide assignments shown. (**D**) Schematic of the covalent structure of RTD-1. The highlighted amino acids correspond to the two 3′ RACE products obtained (*25*), and the color scheme indicates the precursors (Fig. 3, A and C) from which they are derived. (**E**) A theoretical model of RTD-1 obtained by molecular dynamics and energy minimization in water is shown (*19*).
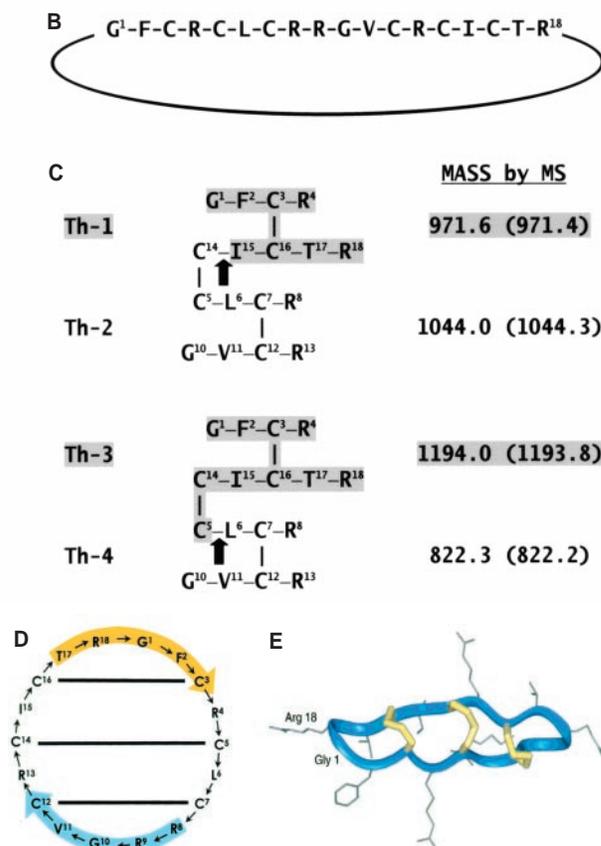
similar in sequence to homologous regions of α-defensin precursors (Fig. 3A) (*27*). Alignment (*16*) of the RTD1a- and RTD1b-deduced precursor sequences with that of HNP-4, the most similar α-defensin, disclosed substantial similarities at the amino acid level (Fig. 3A). However, the covalent structures of mature RTD-1 and HNP-4 (30 amino acids) are markedly dissimilar (*28*). Furthermore, compared to α-defensins, RTD-1 precursors have truncated COOH-terminal segments, encoding only 12 residues after the putative junction between the prosegment and a COOH-terminal dodecapeptide (Fig. 3A).

Genomic clones *RTD1.1* and *RTD1.2*, corresponding to the RTD1a and RTD1b cDNAs, respectively, were isolated from a rhesus macaque genomic library (*29*), confirming that the cDNAs derive from distinct transcriptional units. *RTD1.1* and *RTD1.2* are 93% identical, and the three-exon, two-intron gene structure and organization that they share are very similar to those of the myeloid α-defensin genes characterized previously in humans, rabbits, and guinea pigs (Fig. 3B) (*30*). The close relationship between the RTD-1 and α-defensin genes is also shown by their 88% nucleotide sequence identity with a human α-defensin–related pseudogene (accession U10267). Interestingly, one of the stop codons in this pseudogene corresponds exactly to the position of the stop codons that truncate RTD-1 coding sequences (Fig. 3A).

Comparison of the RTD-1 covalent structure with that of the deduced RTD1a and RTD1b translation products revealed that the cyclic peptide is composed of two nine-residue peptides that are derived separately from the RTD1a and RTD1b precursors. RTD-1 peptide residues 13 to 18 and 1 to 3 correspond to amino acids 65 to 73 from RTD1a, and RTD-1 residues 4 to 12 correspond to RTD1b amino acids 65 to 73 (Fig. 3, A and C). The transformation of the two linear precursors into cyclic RTD-1 requires that two head-to-tail ligation reactions join the constituent nonapeptides by posttranslational reactions not previously recognized (Fig. 3C).

Expression of RTD-1 in myelopoietic elements. The anatomic distribution of RTD-1 gene expression in rhesus macaque tissues was determined by Northern blotting using a probe specific for RTD-1 mRNAs (*31*). Of the 18 organs analyzed, only bone marrow was positive for RTD-1 mRNA (Fig. 4A). The leukocytic lineages in which RTD-1 is expressed were identified by immunohistochemical staining with an anti–RTD-1 antibody (*32*). Dot blot analysis demonstrated that anti–RTD-1 antiserum reacted with natural and synthetic RTD-1 and the oxidized acyclic version of RTD-1, but did not recognize any of the previously characterized α-defensins (HNP-1 through HNP-4) expressed by human leukocytes nor any of the
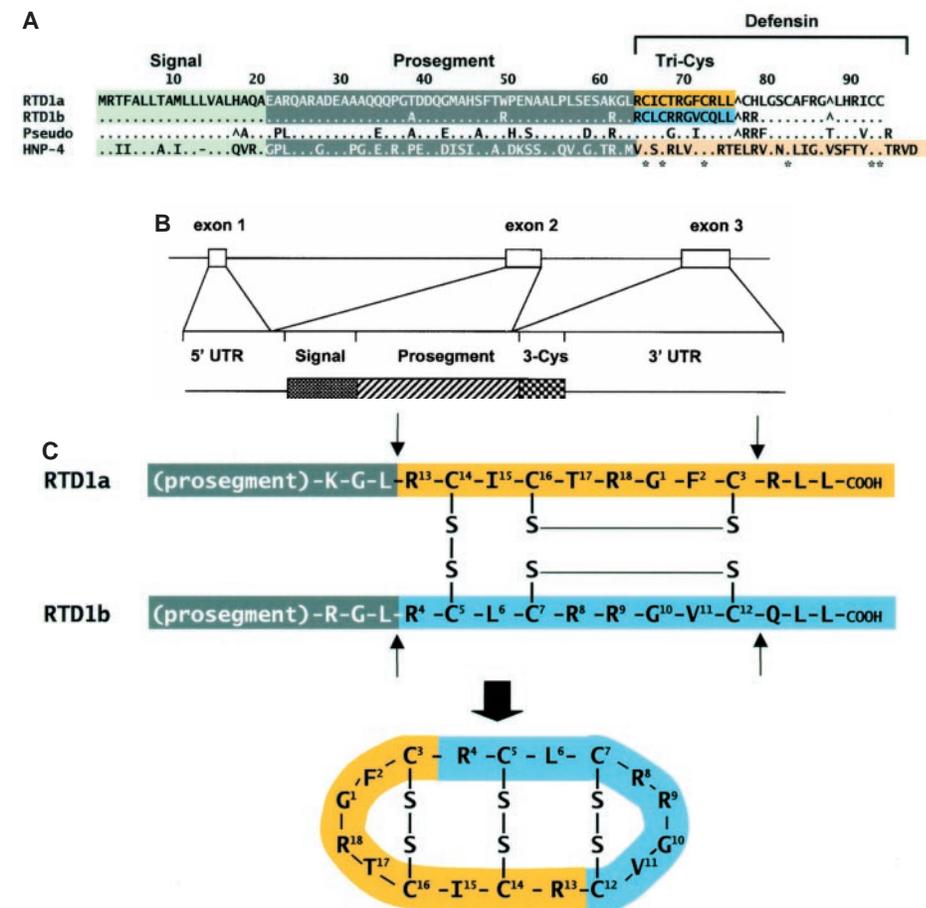

Fig. 3. RTD-1 precursors and genes. (**A**) Deduced RTD1a, RTD 1b, human defensin-like pseudogene (GenBank accession number U10267), and HNP-4 precursor sequences are aligned with in-frame amino acid translations through the mature defensin coding region. Constituent RTD-1 sequences derived from RTD1a and RTD1b (*3-Cys*) are color coded as in Fig. 2D and 3C; white background corresponds to non-translated sequences. Dot characters denote amino acid identity with the RTD1a deduced precursor. The ∧ symbols denote positions of polypeptide chain truncation by termination codons. (**B**) Genomic organization of *RTD1.1* (accession number AF191102) and *RTD1.2* (accession number AF191103). Exons and introns are shown to scale. The bottom line shows the mRNA-prepropeptide relationship. (**C**) Posttranslational processing of RTD-1 precursors. Small arrows denote the boundaries within the RTD1a and RTD1b propeptides that separate each nonapeptide, present in mature RTD-1, from flanking sequences absent in the cyclic structure. The color scheme is consistent with that shown in Figs. 2D and 3A.

rhesus leukocyte α-defensins. Immunostaining of buffy coat leukocytes demonstrated strong, punctate staining in neutrophil cytoplasm, similar to the immunolocalization of neutrophil α-defensins, which are stored in azurophil granules (Fig. 4, B and C). Although less reactive than neutrophils, monocytes were also immunopositive, but lymphocytes and eosinophils were negative. Thus, RTD-1 is expressed in the two major phagocytic cells of the blood.

RTD-1 gene expression and peptide accumulation begin early during granulocyte myelopoiesis. Staining of bone marrow cells with anti–RTD-1 antibody demonstrated immunoreactivity in the cytoplasm of immature myeloid elements (promyelocytes, myelocytes) and in mature neutrophils and monocytes (Fig. 4D). This pattern of expression during myeloid differentiation and the punctate pattern of immu-

nostaining are consistent with the packaging of RTD-1 in azurophil granules.

Microbicidal activity. The in vitro antimicrobial properties of RTD-1 were evaluated in microbicidal assays against a panel of bacterial and fungal test organisms. The broad spectrum of RTD-1 antimicrobial activity was demonstrated in microbicidal assays against Gram-positive bacteria (*S. aureus*, *Listeria monocytogenes*), Gram-negative bacteria (*E. coli* ML 35, *Salmonella typhimurium*), and fungi (*Candida albicans* and *Cryptococcus neoformans*). The viability of each organism was reduced by more than 99% after 2-hour incubations with 2 to 4 μg/ml RTD-1, and higher peptide concentrations (up to 20 μg/ml) effected killing to levels below the detection limit of the assay (Fig. 5, A through C).
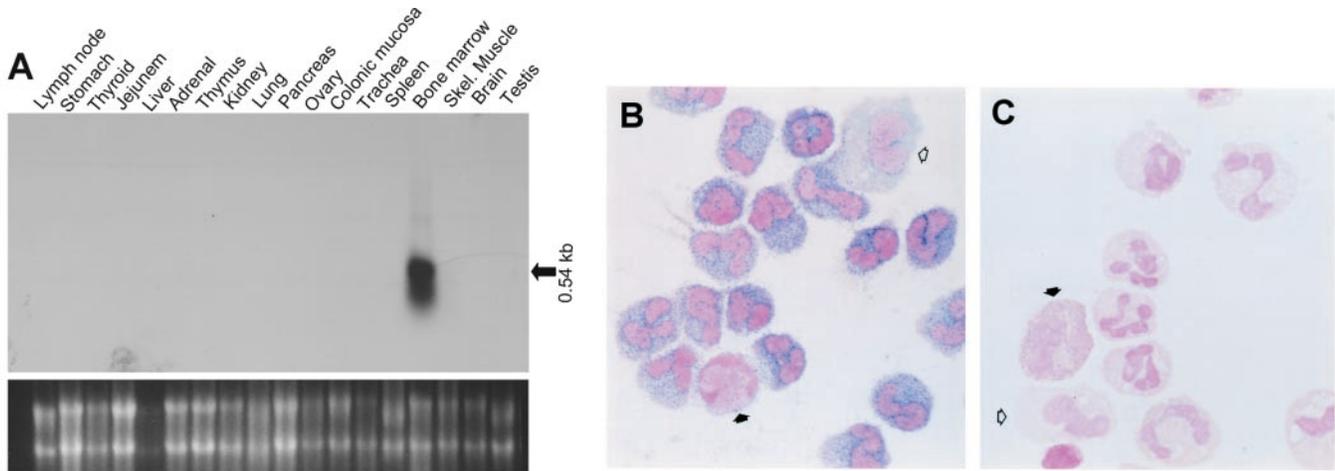
The mechanistic significance of the RTD-1

Fig. 4. RTD-1 mRNA and peptide expression. (**A**) Multiple tissue Northern blot probed with theta defensin–specific PCR product. Lower panel shows ethidium bromide staining of the gel demonstrating RNA integrity and relative loading. (**B**) Immunostaining of peripheral blood buffy coat cells with anti–RTD-1 antibody (*32*) demonstrates strong staining of neutrophils, lighter staining of monocytes (hollow arrow), and no staining of lymphocytes and eosinophils (solid arrow). (**C**) Negative control incubation with buffy coat incubated with RTD-1–preabsorbed antiserum. (**D**) Bone marrow cells were stained with anti–RTD-1 antiserum as in (B). Two representative fields demonstrate strong staining in the cytoplasm of neutrophilic precursors (promyelocyte, Pm; myelocyte, Mc) and segmented neutrophils (hollow arrows). Monocytes (Mo) stain less strongly, and eosinophils (E) are negative.

cyclization was investigated by comparing the antibacterial activities of the cyclic peptide to that of the tridisulfide-containing acyclic analog from which it was produced [supplemental figure 1 (*15*)]. The peptides were tested for activity against *S. aureus* and *E. coli* in an agar diffusion antimicrobial assay (*6*). RTD-1 was three times as active as the acyclic analog against both organisms, indicating that cyclization confers a substantial increase in antimicrobial potency (Fig. 5, D and E).

Previous studies have demonstrated that α- and β-defensin–mediated microbicidal activity is antagonized by increasing the ionic strength of the incubation medium (*33*). In this context, it has been proposed that salt sensitivity of airway β-defensins underlies the susceptibility of cystic fibrosis patients to pulmonary infections (*34*). Therefore, the effect of ionic strength on natural and synthetic RTD-1 staphylocidal activity was determined. Sodium chloride concentrations as high as 150 mM had little effect on the staphylocidal activity of natural or synthetic RTD-1 (Fig. 5F), but the acyclic form of RTD-1 was inhibited nearly completely by 125 mM NaCl. These data demonstrate that the cyclized conformation confers salt-insensitivity to RTD-1. We speculate that under conditions of low (Fig. 5, D and E) and high (Fig. 5F) ionic strength, the cyclic conformer more efficiently binds to and inserts into the target cell envelope than does the acyclic
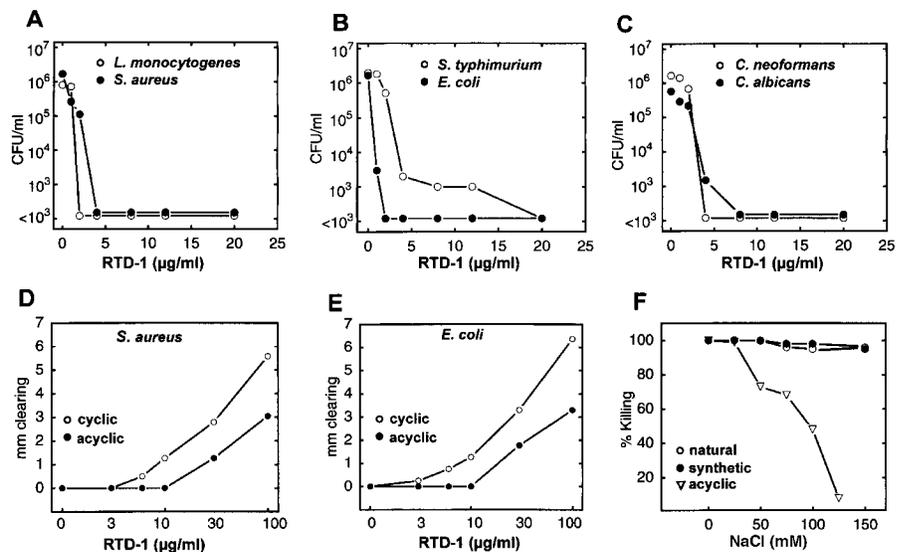

Fig. 5. Microbicidal activity of RTD-1. (**A** through **C**) Each test organism was incubated with RTD-1 at varied concentrations in 10 mM PIPES buffer containing 5 mM glucose for 2 hours at 37°C (*36*). The limit of detection (1 colony per plate) was equal to 1×10^3 colony forming units per milliliter in the incubation mixture. (**D** through **E**) Microbicidal activity of RTD-1 and acyclic RTD-1. Antibacterial activity against *S. aureus* 502a and *E. coli* ML35 was assessed in an agar diffusion assay (*6*). Zones of clearing were measured after 18 hours incubation. (**F**) Salt insensitivity of RTD-1. Killing of *S. aureus* 502a was assessed after 2 hours incubation with 10 μg/ml of natural RTD-1, synthetic RTD-1, or synthetic acyclic RTD-1 in 10 mM PIPES buffer, pH 7.4 containing 5 mM glucose. Incubations mixtures were supplemented with increasing concentrations of NaCl. Percent killing was determined by colony counting.

peptide, which possesses additional charge at both termini.

The broad spectrum of RTD-1 antimicro-

bial activity and its expression in phagocytes raises questions about the evolutionary forces that might have selected for the production of

a cyclic antimicrobial molecule. We speculate that the compact structure of RTD-1 confers resistance to proteases that are abundant in inflammatory exudates, and the lack of NH_2- and COOH-termini eliminates its susceptibility to exopeptidases. In addition, the cyclic conformation confers increased microbicidal activity compared to an acyclic, tridisulfide-containing analog (Fig. 5, D and E), as is required for antibacterial activity in 150 mM NaCl (Fig. 5F).

The cyclic structure of RTD-1 demonstrates that primate cells possess a posttranslational processing pathway capable of head-to-tail peptide chain ligation. The processing pathway that produces the mature RTD-1 from two precursor propeptides requires the proteolytic removal of the prosegments and the COOH-terminal tripeptides from each propeptide (Fig. 3C). While it is possible that disulfide rearrangement may occur in this process, the formation of the one interchain and two intrachain disulfides (Fig. 3C) could position the two hairpin halves of RTD-1 so that the NH_2- and COOH-termini are in proximity for subsequent ligation. It seems likely that the posttranslational pathway employed in the synthesis of RTD-1 is used for the cyclization of other polypeptide precursors.

References and Notes

1. W. F. Broekaert *et al.*, *Crit. Rev. Plant Sci.* **16**, 297 (1997); H. Boman and W. F. Broekaert, *Immunologist* **6**, 234 (1998); J. A. Hoffmann, F. C. Kafatos, C. A. Janeway Jr., R. A. B. Ezekowitz, *Science* **284**, 1313 (1999).
2. A. J. Ouellette and M. E. Selsted, *FASEB J.* **10**, 1280 (1996); T. Ganz and R. I. Lehrer, *Curr. Opin. Hematol.* **4**, 53 (1997); G. Diamond and C. L. Bevins, *Clin. Immunol. Immunopathol.* **88**, 221 (1998).
3. E. D. Stolzenberg, G. M. Anderson, M. R. Ackermann, R. H. Whitlock, M. E. Zasloff, *Proc. Natl. Acad. Sci. U.S.A.* **94**, 8686 (1997); P. K. Singh *et al.*, *ibid.* **95**, 14961 (1998).
4. R. I. Lehrer *et al.*, *J. Clin. Invest.* **84**, 553 (1989).
5. Leukocytes were obtained from anticoagulated whole blood of adult rhesus macaques after erythrocytes were depleted by dextran sedimentation. The cell pellet (6×10^6 cells; 91% neutrophils, 5% mononuclear cells, 4% eosinophils) was snap frozen, suspended in 0.5 ml ice-cold 30% acetic acid, and stirred on melting ice for 18 hours. The suspension was clarified by centrifugation at 4°C, and the supernatant was lyophilized and then dissolved in 0.5 ml methanol:water (80:20). After 6 to 8 hours of stirring at 8°C, the sample was clarified by centrifugation, and the supernatant was lyophilized. The dry powder was dissolved in 0.5 ml 5% acetic acid before RP-HPLC.
6. Antibacterial activity of HPLC fractions, lyophilized and dissolved in 0.01% acetic acid, was determined using an agar diffusion assay [R. I. Lehrer, M. Rosenman, S. S. L. Harwig, R. Jackson, P. Eisenhauer, *J. Immunol. Methods* **137**, 167 (1991)].
7. Sequence analysis was performed by automated Edman degradation with online phenylthiohydantoin amino acid analysis.
8. Y.-Q. Tang, J. Yuan, C. J. Miller, M. E. Selsted, *Infect. Immun.*, in press.
9. Mass spectroscopy (MS) was performed by matrix-assisted laser desorption/ionization–time of flight (MALDI-TOF) on a PE Biosystems Voyager RP mass spectrometer in the linear mode. Samples (1 to 10 pmol) were dissolved in water:acetonitrile (1:1) containing 0.1% trifluoroacetic acid (TFA). All values are reported as the average mass of the nonprotonated species.
10. A. H. Henschen, in *Advanced Methods in Protein Microsequence Analysis*, B. Wittmann-Liebold, J. Salnikow, V. A. Erdman, Eds. (Springer-Verlag, Berlin, 1986), p. 244.
11. Peptide (1 nmol) was dissolved in 24 μl of 1 M methanolic HCl for 48 hours at room temperature. Edman sequencing of two separate reaction mixtures disclosed the sequence shown in Fig. 2A.
12. A 2-nmol sample of *S*-pyridylethylated peptide was digested at 37°C for 10 min with 0.4 μg TPCK trypsin or TLCK α-chymotrypsin in 50 μl of 1% ammonium bicarbonate, pH 8.0. Peptide fragments were purified by C-18 RP-HPLC, giving rise to one predominant peak. Analysis by MALDI-TOF MS (1998.1 obtained; 1997.5 calculated) demonstrated that trypsin cleavage occurred at all five arginines, releasing one arginine and generating a 17-residue, four-stranded oligopeptide connected by three disulfides (Fig. 2C). A 50-pmol sample of the 17-residue oligopeptide was digested with 10 ng of thermolysin in 5 μl of 0.1% TFA (adjusted to pH 7 with 0.1 M ammonium bicarbonate supplemented with 10 mM $CaCl_2$) for 2 hours at 37°C. The reaction was terminated by addition of 5 μl of 0.1% TFA/acetonitrile. One-microliter aliquots of the mixture were analyzed by MALDI-TOF MS as described above. In a separate experiment, ~3 nmol of the 17-mer was digested with thermolysin under similar conditions, and the thermolytic fragments were isolated by HPLC. MALDI-TOF MS analysis of individual peaks confirmed the fragment pattern obtained by MS analysis of the unfractionated digestion mixture.
13. A 2.5-nmol sample of RTD-1 was digested at 37°C for 16 hours with 0.5 μg TPCK trypsin in 50 μl of 0.1 M pyridine acetate, pH 6.4. The digest was fractionated by RP-HPLC, giving rise to one predominant peak. Analysis by MALDI-TOF MS (1998.1 obtained; 1997.5 calculated) demonstrated that trypsin cleavage occurred at all five arginines, releasing one arginine and generating a 17-residue, four-stranded oligopeptide connected by three disulfides (Fig. 2C). A 50-pmol sample of the 17-residue oligopeptide was digested with 10 ng of thermolysin in 5 μl of 0.1% TFA (adjusted to pH 7 with 0.1 M ammonium bicarbonate supplemented with 10 mM $CaCl_2$) for 2 hours at 37°C. The reaction was terminated by addition of 5 μl of 0.1% TFA/acetonitrile. One-microliter aliquots of the mixture were analyzed by MALDI-TOF MS as described above. In a separate experiment, ~3 nmol of the 17-mer was digested with thermolysin under similar conditions, and the thermolytic fragments were isolated by HPLC. MALDI-TOF MS analysis of individual peaks confirmed the fragment pattern obtained by MS analysis of the unfractionated digestion mixture.
14. Y.-Q. Tang and M. E. Selsted, *J. Biol. Chem.* **268**, 6649 (1993).
15. Supplemental material can be found at www.sciencemag.org/feature/data/1041865.shl
16. S. F. Altschul *et al.*, *Nucleic Acids Res.* **25**, 3389 (1997).
17. V. N. Kokryakov *et al.*, *FEBS Lett.* **327**, 231 (1993); C. Q. Zhao, T. Ganz, R. I. Lehrer, *FEBS Lett.* **368**, 197 (1995); R. L. Fahrner *et al.*, *Chem. Biol.* **3**, 543 (1996).
18. M. Zanetti, R. Gennaro, D. Romeo, *FEBS Lett.* **374**, 1 (1995).
19. A three-dimensional model of RTD-1 was constructed using the Insight II program with the consistent valence force field based on the backbone conformation of residues 6 to 15 found in the solution structure of PG-1 (entry 1pg1 in the Brookhaven Protein Database). The molecule was placed into a 25.0 Å radius sphere of water. After energy minimization, a 250-ps molecular dynamics simulation was carried out at 300 K. The backbone atom root-mean-square fluctuation around the mean structure reached a steady state in the last 200 ps. Subsequent energy minimization of the average structure resulted in the structure shown in Fig. 2E.
20. R. Derua, K. R. Gustafson, L. K. Pannell, *Biochem. Biophys. Res. Commun.* **228**, 632 (1996).
21. K. R. Gustafson *et al.*, *J. Am. Chem. Soc.* **116**, 9337 (1994).
22. J. P. Tam, Y. A. Lu, J. L. Yang, K. W. Chiu, *Proc. Natl. Acad. Sci. U.S.A.* **96**, 8913 (1999).
23. A. Galvez, G. Gimenez-Gallego, M. Maqueda, E. Valdivia, *Antimicrob. Agents Chemother.* **33**, 437 (1989); M. Martinez-Bueno *et al.*, *J. Bacteriol.* **176**, 6334 (1994).
24. A. Blond *et al.*, *Eur. J. Biochem.* **259**, 747 (1999).
25. A degenerate oligonucleotide (5'-CGAGGNGTNT-GYMGNTGYATHTG-3', 1536-fold degenerate) corresponding to residues G^{10}VCRCIC of RTD-1 was one of several sense primers used for 3' RACE (*35*). Amplification products were subcloned and sequenced. Two of the amplified products contained sequences that encoded TRGFCRLL(stop) and RRGVCQLL(stop), corresponding to the COOH-termini of RTD1a and RTD1b, respectively. Single-letter abbreviations for the amino acid residues are as follows: A, Ala; C, Cys; D, Asp; E, Glu; F, Phe; G, Gly; H, His; I, Ile; K, Lys; L, Leu; M, Met; N, Asn; P, Pro; Q, Gln; R, Arg; S, Ser; T, Thr; V, Val; W, Trp; and Y, Tyr.
26. A cDNA library was prepared from bone marrow RNA in Lambda ZAP II (Stratagene) using the Smart cDNA cloning system (CLONTECH), and screened with ^{32}P-labeled 3' RACE products (*25*). Of 1.6×10^6 clones screened, 15 were purified and sequenced.
27. N. Y. Yount *et al.*, *J. Immunol.* **155**, 4476 (1995); T. Ganz and R. I. Lehrer, *Curr. Opin. Hematol.* **4**, 53 (1997).
28. S. H. White, W. C. Wimley, M. E. Selsted, *Curr. Opin. Struct. Biol.* **5**, 521 (1995).
29. A rhesus macaque genomic library constructed in EMBL3 was purchased from CLONTECH and ~1 × 10^6 plaque-forming units were screened with a combined RTD1a and RTD1b cDNA probe by standard procedures. Of the >50 double-positive clones, 10 were selected at random for further purification and analysis. Genomic clones coding for RTD1a and RTD1b were distinguished by Southern (DNA) blot hybridization of polymerase chain reaction (PCR) products using sequence specific primers. Restriction analysis demonstrated that all 10 clones were unique. Appropriate PCR products were inserted in pCR 2.1 vector (Invitrogen) and sequenced.
30. M. E. Selsted and A. J. Ouellette, *Trends Cell Biol.* **5**, 114 (1995).
31. RNA was extracted from snap-frozen tissues, and 40 μg of each sample was resolved on a 1.2% agarose-formaldehyde gel, and transferred to a membrane. The membrane was hybridized with probes specific for RTD1a (nucleotides 241–325) and RTD1b (nucleotides 236−320) generated by PCR. The specificity of the probes for RTD-1 was demonstrated by their ability to hybridize selectively RTD-1 sequences and their lack of hybridization to rhesus myeloid α-defensin cDNAs.
32. A 1.2-mg sample of acyclic RTD-1 was conjugated to 1.2 mg of ovalbumin in 2.4 ml of 0.1 M sodium phosphate, pH 7.4, containing 0.1% glutaraldehyde with stirring for 18 hours. The reaction was quenched by addition of 0.3 M glycine hydrochloride, dialyzed against water, and split for immunization of two New Zealand White rabbits. The antiserum from both rabbits was ~1:1000, as determined by ELISA (enzyme-linked immunosorbent assay) using acyclic RTD-1 conjugated to goat γ-globulin as the target antigen. Cytospin preparations of peripheral blood leukocytes and bone marrow cells, fixed with 4% paraformaldehyde, were preincubated with avidin, biotin, and Fc receptor blocker, then incubated with 1:100 rabbit anti–RTD-1 antiserum and developed with biotinylated goat anti-rabbit immunoglobulin-G, washed and incubated with avidin/biotin/glucose oxidase complex that was visualized with nitroblue tetrazolium. Negative control incubations were performed with anti–RTD-1 antiserum that was preabsorbed with 1 mg of synthetic acyclic RTD-1 per milliliter of antiserum.
33. M. E. Selsted, D. Szklarek, R. I. Lehrer, *Infect. Immun.* **45**, 150 (1984); R. Bals, M. T. Goldman, J. M. Wilson, *ibid.* **66**, 1225 (1998); E. V. Valore *et al.*, *J. Clin. Invest.* **101**, 1633 (1998).
34. J. J. Smith, S. M. Travis, E. P. Greenberg, M. J. Welsh, *Cell* **85**, 229 (1996); M. J. Goldman *et al.*, *Cell* **88**, 553 (1997).
35. M. A. Frohman, in *PCR Protocols: A Guide to Methods and Applications*, M. A. Innis, D. H. Gelfand, J. J. Sninsky, T. J. White, Eds. (Academic Press, San Diego, CA, 1990), p. 28.
36. M. E. Selsted, in *Genetic Engineering: Principles and Methods*, vol. 15, J. K. Setlow, Ed. (Plenum, New York, 1993), p. 131.
37. Supported in part by NIH grant AI22931 and Biosource Technologies, Inc (M.E.S.), NIH grants DK44632 and DK33506 (A.J.O.), and NIH grant RR00169 (C.J.M.). We thank H. Truong, B. Hoover, P. Tran, D. Lu, and Y. Wang for expert technical assistance, as well as A. Fowler at the University of California Los Angeles Microsequencing Core Facility and A. Henschen, Director of the University of California Irvine Microchemical Core Facility.